

## SUPPORTING INFORMATION

### Selective Synthesis of LaF<sub>3</sub> and NaLaF<sub>4</sub> Nanocrystals via

### Lanthanide Ion Doping<sup>†</sup>

Li Nie,<sup>\*a</sup> Yuxing Shen,<sup>\*a</sup> Xi Zhang,<sup>a</sup> Xiuwen Wang,<sup>a</sup> Botong Liu,<sup>a</sup> Yangbo Wang,<sup>a</sup> Yue Pan,<sup>b</sup> Xiaoji Xie,<sup>\*a</sup>  
Ling Huang<sup>\*a</sup> and Wei Huang<sup>a</sup>

*<sup>a</sup>Key Laboratory of Flexible Electronics (KLOFE) & Institute of Advanced Materials (IAM),  
Jiangsu National Synergetic Innovation Center for Advanced Materials (SICAM), Nanjing Tech  
University (NanjingTech), 30 South Puzhu Road, Nanjing 211816, P. R. China. E-mail:  
iamxjxie@njtech.edu.cn, iamlhuang@njtech.edu.cn, iamwhuang@njtech.edu.cn*

*<sup>b</sup>School of Chemistry and Chemical Engineering, Inner Mongolia University, 235 West Daxue Road,  
Hohhot 010021, P. R. China*

## Experimental section

### Materials

$\text{La}(\text{NO}_3)_3 \cdot 6\text{H}_2\text{O}$ ,  $\text{Ce}(\text{NO}_3)_3 \cdot 6\text{H}_2\text{O}$ ,  $\text{Pr}(\text{NO}_3)_3 \cdot 6\text{H}_2\text{O}$ ,  $\text{Nd}(\text{NO}_3)_3 \cdot 6\text{H}_2\text{O}$ ,  $\text{Ho}(\text{NO}_3)_3 \cdot 6\text{H}_2\text{O}$ ,  $\text{Eu}(\text{NO}_3)_3 \cdot 6\text{H}_2\text{O}$ ,  $\text{Gd}(\text{NO}_3)_3 \cdot 6\text{H}_2\text{O}$ ,  $\text{Tb}(\text{NO}_3)_3 \cdot 6\text{H}_2\text{O}$ ,  $\text{Dy}(\text{NO}_3)_3 \cdot 6\text{H}_2\text{O}$ ,  $\text{Yb}(\text{NO}_3)_3 \cdot 5\text{H}_2\text{O}$ ,  $\text{Er}(\text{NO}_3)_3 \cdot 6\text{H}_2\text{O}$ ,  $\text{Tm}(\text{NO}_3)_3 \cdot 5\text{H}_2\text{O}$ ,  $\text{Sm}(\text{NO}_3)_3 \cdot 6\text{H}_2\text{O}$ , and  $\text{Lu}(\text{NO}_3)_3 \cdot 6\text{H}_2\text{O}$  with purity >99.99% were purchased from Jinan HH. Ethylene glycol (EG),  $\text{NaNO}_3$  and  $\text{NH}_4\text{F}$  were all analytical grade reagents, respectively purchased from Shanghai Shisihewei Chemical CO., Sinopharm Chemical Reagent Limited Corporation, and Shanghai Shenbo Chemical CO..

### Characterization

All samples were measured by powder X-ray diffraction (XRD) on a Rigaku D/max 2550, which under the monochromatized  $\text{Cu K}\alpha$  radiation ( $\lambda = 0.15418 \text{ nm}$ ), Transmission electron microscopy (TEM) images were recorded on a Hitachi 7700 transmission electron microscope at an acceleration voltage of 100 kV. The inductively coupled plasma mass spectroscopy (ICP-MS) analysis was performed on a PE Optima 5300DV spectrometer. Both DC and UP luminescence spectrum were recorded on a Hitachi F-4600 spectrometer equipped with a Xe lamp and an external continuous diode 980 nm laser.

### Synthesis of hexagonal $\text{LaF}_3$ and hexagonal $\text{NaLaF}_4$ nanocrystals

Lanthanide-doped hexagonal  $\text{LaF}_3$  and hexagonal  $\text{NaLaF}_4$  nanocrystals were synthesized by a solvothermal method. Briefly, 0.65 mmol  $\text{RE}(\text{NO}_3)_3$  was dissolved in 15 mL ethylene glycol (EG). After vigorous stirring for 30 minutes,  $\text{NaNO}_3$  and  $\text{NH}_4\text{F}$  were introduced into the solution with the mole ratio of  $\text{RE}^{3+}:\text{Na}^+:\text{F}^-$  at 1:3:30. After 30 mins further stirring, the resulting solution was transferred into a 25 mL sealed Teflon autoclave and maintained at 180 °C for 12 h. The precipitates were collected by centrifugation and washed several times with ethanol and deionized water after the autoclave was cooled down to room temperature. The products were dried in at 70 °C for 24 h and stored for further use. Controllable synthesis of hexagonal  $\text{NaLaF}_4$  and hexagonal  $\text{LaF}_3$  under different doping conditions. Similarly, other lanthanides also are used as dopants in the same synthesis procedures.

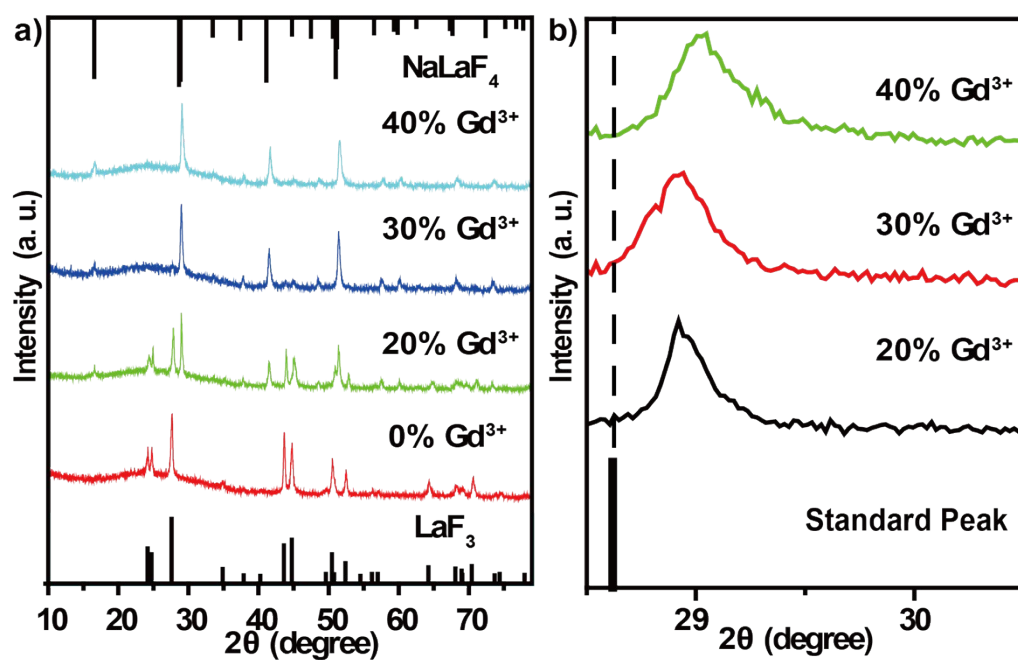


**Fig. S1** (a) XRD patterns of the final products at 0, 20, 30, and 40 mol% Gd<sup>3+</sup> doping. (b) Details of the right shift of the characteristic XRD peak of NaLaF<sub>4</sub> nanocrystals at 28.7° when Gd<sup>3+</sup> worked as dopant ions.

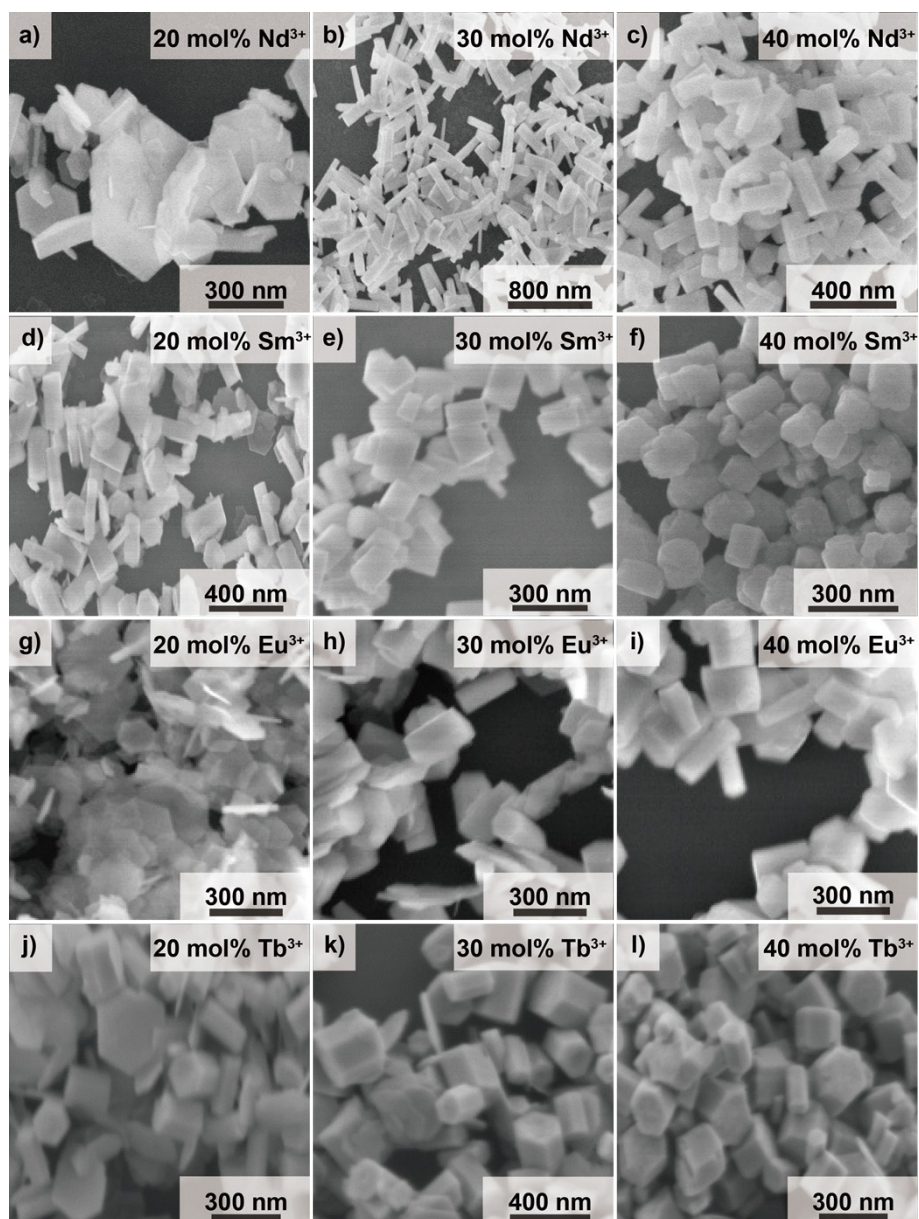


**Fig. S2** SEM images of  $\beta$ -NaLaF<sub>4</sub> nanocrystals doped with (a-c) Nd<sup>3+</sup>, (d-f) Sm<sup>3+</sup>, (g-i) Eu<sup>3+</sup>, and (j-l) Tb<sup>3+</sup> at varying concentrations.

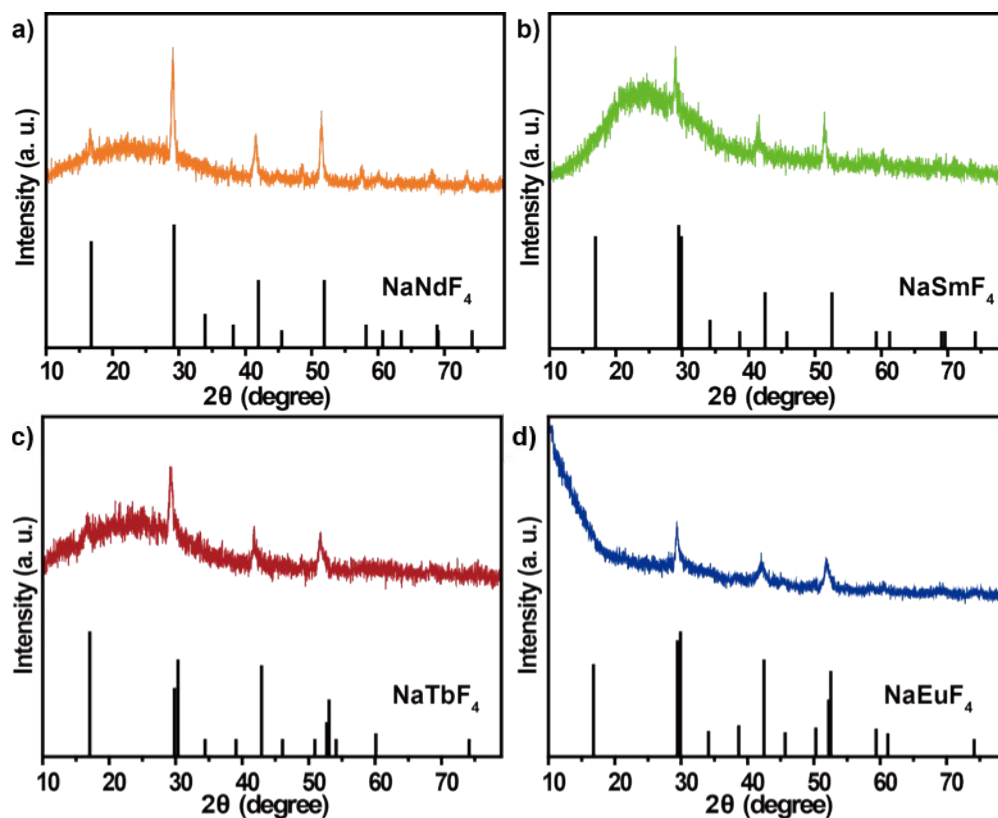


**Fig. S3** XRD patterns of  $\beta$ - $\text{NaMF}_4$  (M = Nd, Sm, Eu, and Tb) nanocrystals doped with 60 mol% (a)  $\text{Nd}^{3+}$ , (b)  $\text{Sm}^{3+}$ , (c)  $\text{Tb}^{3+}$ , and (d)  $\text{Eu}^{3+}$ .

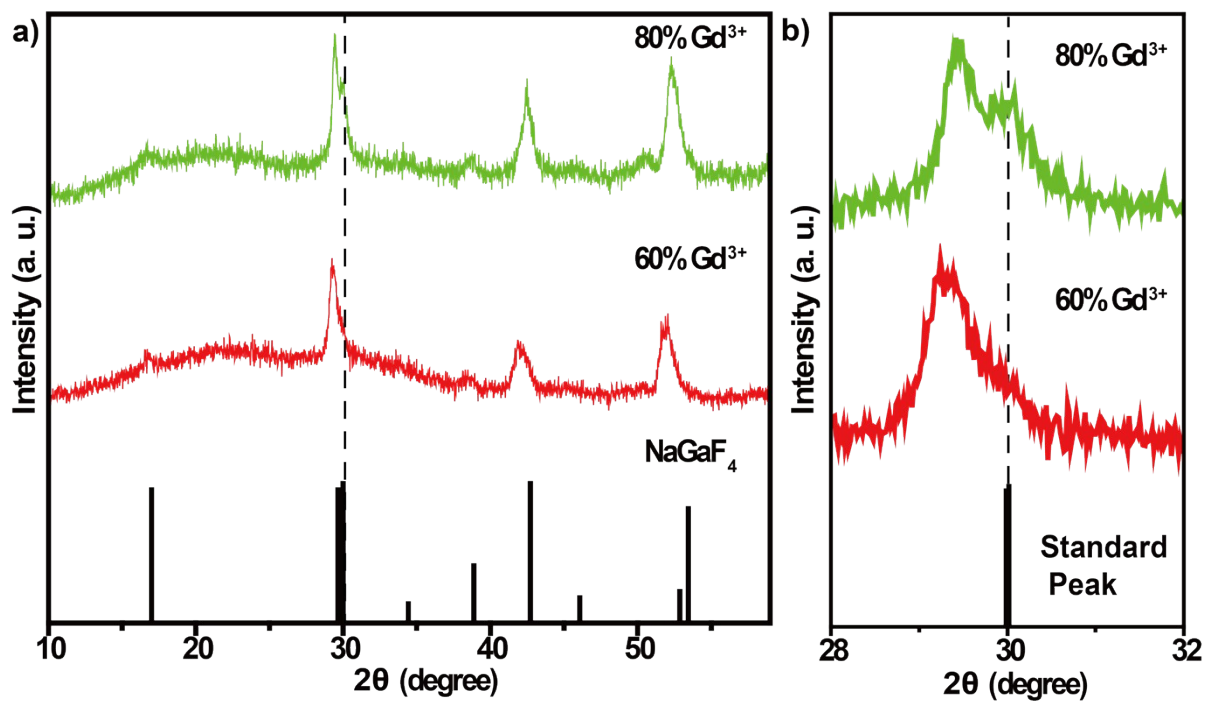


**Fig. S4** (a) XRD patterns of the final products at 60 and 80 mol%  $\text{Gd}^{3+}$  doping. (b) Details of the left shift of the characteristic XRD peak of  $\text{NaGaF}_4$  nanocrystals at  $30^\circ$  when  $\text{La}^{3+}$  worked as dopant ions.

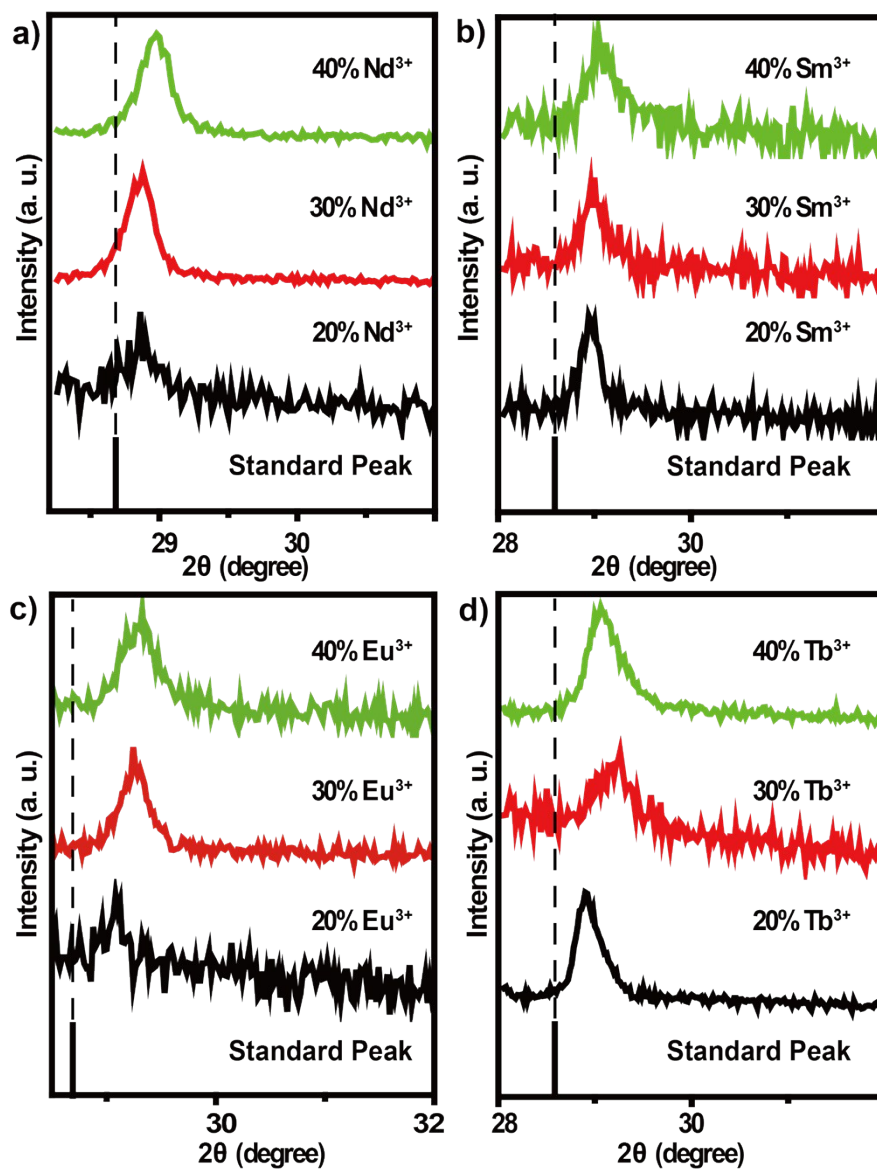


**Fig. S5** Details of the right shift of the characteristic XRD peaks of  $\beta$ -NaLaF<sub>4</sub> nanocrystals doped with (a) Nd<sup>3+</sup>, (b) Sm<sup>3+</sup>, (c) Eu<sup>3+</sup>, and (d) Tb<sup>3+</sup> at varying concentrations.

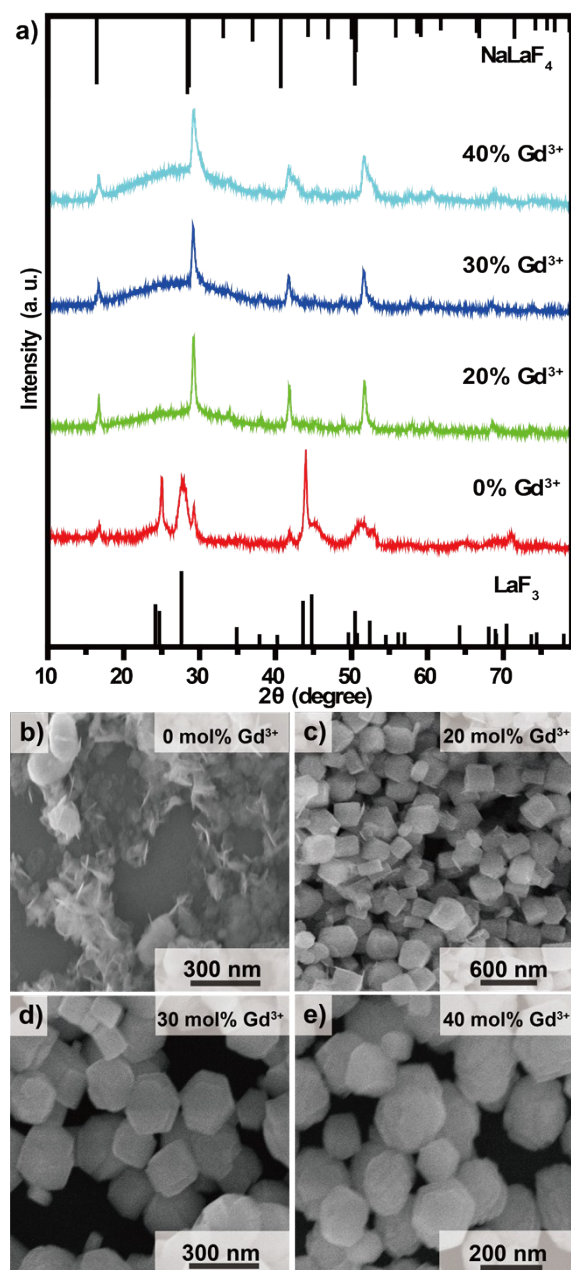


**Fig. S6** (a) XRD patterns and (b-e) SEM images of nanocrystals at varying  $\text{Gd}^{3+}$  doping concentrations. Co-doping of  $\text{Yb}^{3+}$  (18 mol%) and  $\text{Er}^{3+}$  (2 mol%) is for the studies of both the doping effect on the nanocrystal growth mechanism and upconversion luminescence.



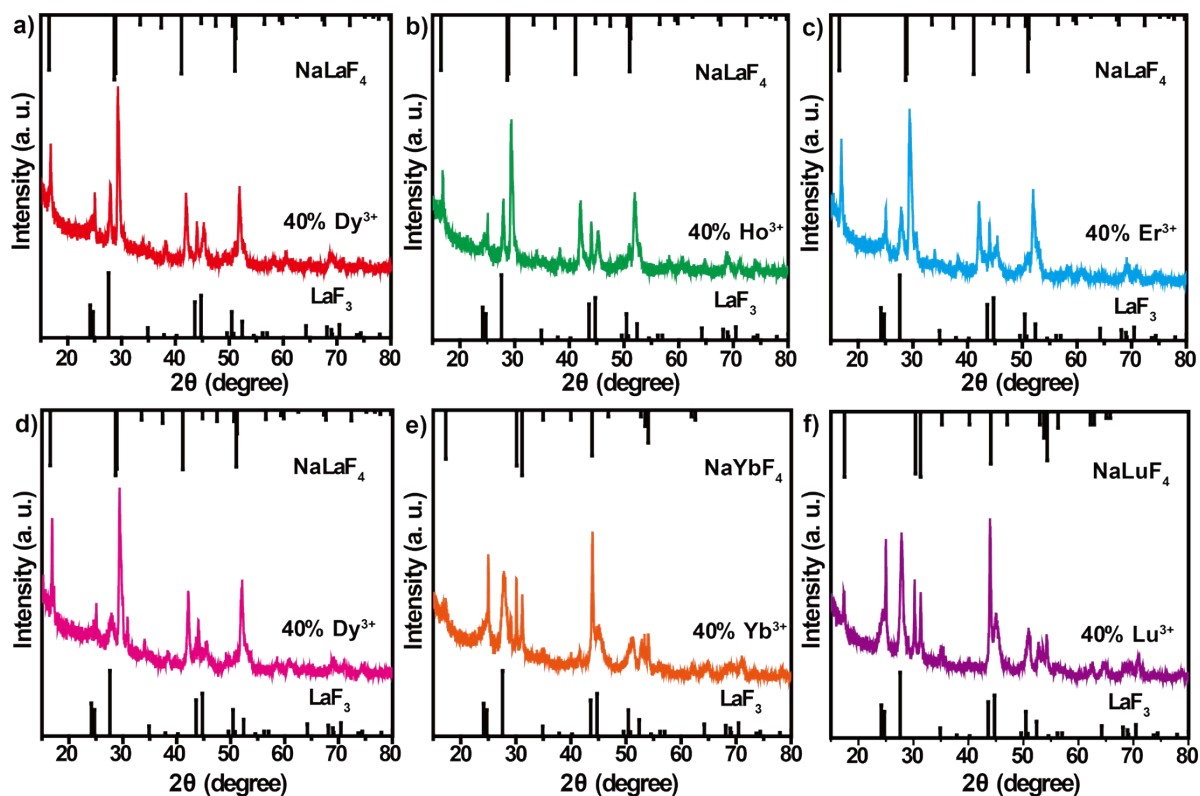


**Fig. S7** XRD patterns of products doped with (a)  $\text{Dy}^{3+}$ , (b)  $\text{Ho}^{3+}$ , (c)  $\text{Er}^{3+}$ , (d)  $\text{Tm}^{3+}$ , (e)  $\text{Yb}^{3+}$ , and (f)  $\text{Lu}^{3+}$  at 40 mol% doping concentrations, which are the mixture of  $\text{LaF}_3\text{:Ln}$  and  $\text{NaLaF}_4\text{:Ln}$  ( $\text{Ln} = \text{Dy}, \text{Ho}, \text{Er}, \text{Tm}, \text{Yb}, \text{and Lu}$ ) nanocrystals.

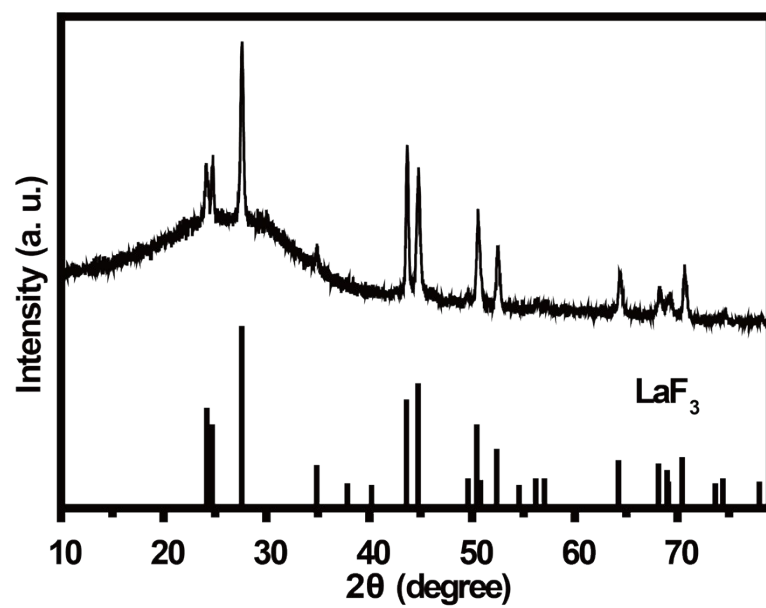


**Fig. S8** XRD patterns of the nanocrystals obtained after post-doping of  $\text{Gd}^{3+}$  into the reaction system with pre-synthesized  $\text{LaF}_3$  nanocrystals.